J Neurogastroenterol Motil, Vol. 28 No. 3 July, 2022
pISSN: 2093-0879 eISSN: 2093-0887
https://doi.org/10.5056/jnm21074
Journal of Neurogastroenterology and Motility

Original Article

A Potential Role of Cholinergic Dysfunction on Impaired Colon Motility in Experimental Intestinal Chagas Disease

Mayra F Ricci,[1] Samantha R Béla,[1,2] Joana L Barbosa,[5] Michele M Moraes,[1] Ana L Mazzeti,[3] Maria T Bahia,[4] Laila S Horta,[5] Helton da C Santiago,[5] Jader S Cruz,[5] Luciano dos S A Capettini,[6] and Rosa M E Arantes[1]*

[1]Departamento de Patologia Geral, Instituto de Ciências Biológicas, Universidade Federal de Minas Gerais, Belo Horizonte, Minas Gerais, Brasil; [2]Instituto de Ciências Exatas e Biológicas, Universidade Federal de Ouro Preto, Ouro Preto, Minas Gerais, Brasil; [3]Laboratório de Biologia Celular, Instituto Oswaldo Cruz, Fundação Oswaldo Cruz, Rio de Janeiro, Brasil; [4]Escola de Medicina & Núcleo de Pesquisas em Ciências Biológicas, Universidade Federal de Ouro Preto, Ouro Preto, Minas Gerais, Brasil; [5]Departamento de Bioquímica e Imunologia, Universidade Federal de Minas Gerais, Belo Horizonte, Minas Gerais, Brasil; and [6]Departamento de Farmacologia, Instituto de Ciências Biológicas, Universidade Federal de Minas Gerais, Belo Horizonte, Minas Gerais, Brasil

Background/Aims
Chagasic megacolon is caused by *Trypanosoma cruzi*, which promotes in several cases, irreversible segmental colonic dilation. This alteration is the major anatomic-clinical disorder, characterized by the enteric nervous system and muscle wall structural damage. Herein, we investigate how *T. cruzi*-induced progressive colonic structural changes modulate the colonic contractile pattern activity.

Methods
We developed a murine model of *T. cruzi*-infection that reproduced long-term modifications of the enlarged colon. We evaluated colonic and total intestinal transit time in animals. The patterns of motor response at several time intervals between the acute and chronic phases were evaluated using the organ bath assays. Enteric motor neurons were stimulated by electric field stimulation. The responses were analyzed in the presence of the nicotinic and muscarinic acetylcholine receptor antagonists. Western blot was performed to evaluate the expression of nicotinic and muscarinic receptors. The neurotransmitter expression was analyzed by real-time polymerase chain reaction.

Results
In the chronic phase of infection, there was decreased intestinal motility associated with decreased amplitude and rhythmicity of intestinal contractility. Pharmacological tests suggested a defective response mediated by acetylcholine receptors. The contractile response induced by acetylcholine was decreased by atropine in the acute phase while the lack of its action in the chronic phase was associated with tissue damage, and decreased expression of choline acetyltransferase, nicotinic subunits of acetylcholine receptors, and neurotransmitters.

Conclusions
T. cruzi-induced damage of smooth muscles was accompanied by motility disorders such as decreased intestinal peristalsis and cholinergic system response impairment. This study allows integration of the natural history of Chagasic megacolon motility disorders and opens new perspectives for the design of effective therapeutic.
(J Neurogastroenterol Motil 2022;28:483-500)

Key Words
Acetylcholine; Enteric nervous system; Gastrointestinal motility; Megacolon; *Trypanosoma cruzi*

Received: April 8, 2021 Revised: July 21, 2021 Accepted: October 11, 2021

*Correspondence: Rosa M E Arantes, MD, PhD
Instituto de Ciências Biológicas, Departamento de Patologia Geral, Universidade Federal de Minas Gerais, Mail Box 486, Belo Horizonte, MG 31270-901, Brasil
Tel: +55-31-3409-2896/2878, Fax: +55-31-3409-2879, E-mail: rosa.esteves.arantes@gmail.com/rosa@icb.ufmg.br

Introduction

The intestinal Chagas disease (CD) pathogenesis includes damage to the enteric nervous system (ENS) possibly associated with yet not well-comprehended changes in intestinal motility and enteric neurons' neurotransmitters culminating with the formation of megacolon, it is characterized by an increase in the thickness, dilation, and sometimes elongation, of the intestinal wall. The ENS damage causes subsequent ganglionic and intramuscular denervation.[1-3]

The main symptom associated with Chagasic megacolon is chronic constipation.[4-7] By manometry studies, it was demonstrated that colonic basal motility is lower in Chagasic patients when compared to normal subjects. Some studies, in the Chagasic patients, showed a reduced relaxation of the internal anal sphincter.[6,8-11] However, the mechanisms involved in intestinal dysmotility related to CD are poorly understood.

The mechanism of colonic motility involves activation of the autonomic nervous system which includes extrinsic parasympathetic, sympathetic nerves, and interneurons, that coordinate excitatory and inhibitory response of the enteric motor neurons.[12] The two main components responsible for peristalsis are acetylcholine, which promotes muscular contraction, and nitric oxide (NO), which induces intestinal smooth muscle relaxation.[13] Previously, we observed selective preservation of neuronal nitric oxide synthase (nNOS)-positive neurons to detriment of cholinergic neurons in the same model.[3] Also, some authors described evidence for enhanced inhibitory neurotransmission in the human.[14,15] So, the structural elements in the *tunica muscularis* are affected by *Trypanosoma cruzi* that induces potential alterations in the pattern of the intestinal motility seen on megacolon development.

Even though the advanced studies analyzing enteric neural circuits,[16-19] the integration between the structural events and motor components is still poorly understood during CD, and it is difficult to study even in experimental models. Altered levels of acetylcholine (Ach) or modified receptors expression and function in the ENS could explain dysfunction of the cholinergic system in the Chagasic megacolon.[20]

Here we studied the effects of *T. cruzi*-induced inflammation and denervation in these circuits, using a long-term animal model that reproduced the colonic changes' progression culminating in megacolon formation.[21] We performed studies of motility in vivo and correlated with pharmacological tests ex vivo to evaluate how CD progressive intestinal structural changes in ENS, neurotransmitters expression, intestinal smooth muscle phenotype, and contractile machinery may correlate to dysmotility disorders.

Our goal is to investigate how experimental *T. cruzi*-induced intestinal lesions interfere with peristalsis and gastrointestinal (GI) motility and possible dysfunction of muscarinic and nicotinic receptors in the morbid symptoms of human megacolon.[8,22]

Materials and Methods

In vivo and ex vivo animal experiments complied with the principles established by guidelines and the Brazilian Practice Directive for the Care and Use of Animals for Scientific and Didactic Purposes (Notice MCTI No. 1 - CONCEA/MCTI). Animal studies comply with the ARRIVE guidelines under protocol number 262/2016 and 31/2017.[23,24]

Mice

Female Swiss mice, 4-week old, with approximately 30 g weight were used. The animals were euthanized by cervical dislocation performed by trained individuals, as pharmacological methods would interfere with the aims of the present study.

Trypanosoma cruzi Infection Experimental Protocols

Mice infection was performed by intraperitoneal injection with 50 000 blood trypomastigotes of *T. cruzi* strain Y, as described before.[25] All animals were inoculated at the Laboratory of Parasitic Diseases. The efficacy of infection was evaluated by the presence of parasites in fresh blood 4 days after inoculation. At 15 months post-infection (m.p.i), parasite DNA by real-time polymerase chain reaction (PCR) was detected in infected mice used in the experiments.

Female Swiss mice were randomly and blindly divided into 2

groups.[3] The non-infected control group was composed of a control acute phase (CAP) and a control chronic phase (CCP) groups. Following Ricci and collaborators' protocols,[3] the infected group was composed of the infected acute phase (IAP) and chronic phase (ICP). IAP group euthanized at 11 days post-infection (d.p.i) before manifestating signals of the disease. ICP group was treated orally with a single dose of 500 mg/kg body weight of benznidazole (Pharmaceutical Laboratory of the State of Pernambuco, Lafepe, Brazil) at 11 d.p.i. and maintained up to 15 months post-infection (m.p.i.). The animals of ICP were euthanized at 3, 7, 12, and 15 m.p.i. (ICP3, ICP7, ICP12, and ICP15 groups, respectively); thus, the motility measures and electrophysiology assays were carried out throughout the development of megacolon. The non-infected age-matched chronic control groups were maintained in the same condition and euthanized at appropriate months indicated as CCP3, CCP7, CCP12, and CCP15. Two independent experiments were performed.

Aiming for the rational use of animals, we use the same group of animals for in vivo motility studies and histopathological analysis. Another group of animals was used for PCR and Western blot assays, and for evaluating the patterns of responses induced by electrical field stimulation (EFS, Hz) and the amplitude of contractility induced by inhibition of muscarinic, neural, and nicotinic pathways in organ bath ex vivo, and for Western blot analysis.

In Vivo Motility Studies

Total gastrointestinal transit assay

The solution with 300 μL of 6% carmine red dye solution (in distilled water containing 0.5% methylcellulose) (Merck, New York, NY, USA) was administrated by intragastric gavage in mice. After that, the animals were placed into individual cages. To facilitate the detection of carmine dye in the fecal pellets, a white sheet of paper covered the cage bottom. The gavage was recorded as time 0. After gavage, we monitored fecal pellets every 10 minutes for the presence of carmine red. The total GI transit time (total transit time) represents the interval between time 0 and the time of the first observance of carmine red dye in the stool.

Colon motility assay

Adult mice were anesthetized with isoflurane (BioChimico, Rio de Janeiro, Brazil) a lubricated (glycerin [G1005.01.BJ]; LabSynth, Diadema, SP, Brazil) glass rod was used to insert glass bead (3 mm in diameter; Z143928; Sigma-Aldrich, St. Louis, MO, USA) into the rectum, 2 cm from the anal verge. The time in seconds required to eject the bead was measured as an estimate of colonic transit time.[26-28]

We also evaluated the colonic and total intestinal motility in mice previously treated with the cholinesterase inhibitor pyridostigmine administered through intragastric gavage (1 mg/kg; Sigma-Aldrich).

Histopathological analysis and semi-quantitative score

The animals were euthanized by cervical dislocation performed by trained individuals. The histopathological analysis was performed by the technique as previously described.[29] The rolls were then fixed in formaldehyde (10%), prepared for paraffin-embedding, and submitted to microtomy and H&E staining. The score was plotted on a blue color scale, where lighter colors indicate less severity and darker colors indicate greater severity. Samples of 5 representative animals from all infected groups were evaluated at all time intervals. We graphically represented the attributed score based on the intensity of the changes as 0-absence (white), 1-small changes (light blue), 2-intermediate changes (blue), and 3-intense changes (navy blue).

Under a bright-field microscope, the colon extension (H&E stained) was subjected to analysis of inflammatory foci/area: absent, score 0; 32-35 foci/area, score 2; 36-84 foci/area, score 3. The smooth muscle degenerative changes were classified as absent, score 0; slight changes, score 1; moderate changes, score 2; severe changes, score 3; by examining 8-10 fields under 20× objective (each field measured 79 265.56 μm^2). We also attributed values for parasitism (parasite DNA/25 μg of colon tissue): < 174, score 1; 174-329, score 2; 330-131 000, score 3; and the wall thickness (inner layer thickness): 5-6 mm, score 1; 7-8 mm, score 2 (please refer to Fig. 1A-E, for histopathology). In Figure 1G each row represents a time point and each column indicates the parameters for the group in question.

Imaging

Photographic documentation and morphometric analysis were obtained using the Olympus BX51 direct light optical microscope equipped with Image-Pro Express 4.0 software (Media Cybernetics, Rockville, MD, USA) with a resolution of 1392 × 1040 pixels. Images were transferred via a Cool SNAP-Proof Color camcorder to a computer-attached video system using Image-Pro Express version 4.0 for Windows (Media Cybernetics).

Morphometric analysis

Images were obtained with 10 × objective, of the full length of

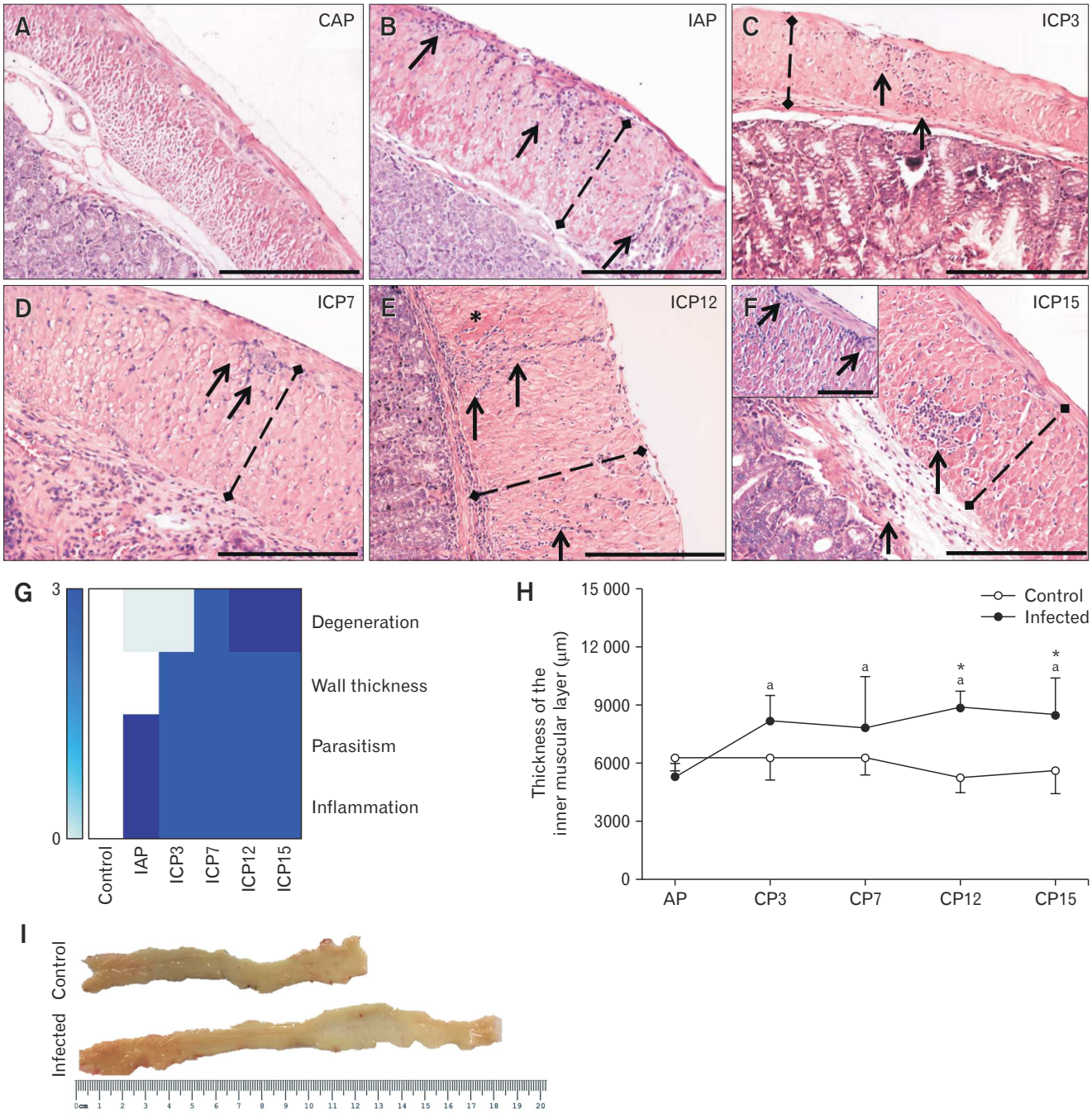

Figure 1. Natural history and pathological anatomy of the murine megacolon. Control and infected groups were evaluated in the acute phase (AP; 11 days) and chronic phases (CP; 3, 7, 12, and 15 months post-infection [m.p.i]) of *Trypanosoma cruzi* infection. (A) control acute phase (CAP), (B) infected acute phase (IAP), (C) infected chronic phase 3 m.p.i. (ICP3), (D) infected chronic phase 7 m.p.i. (ICP7), (E) control chronic phase 12 m.p.i. (ICP12), (F) control chronic phase 15 m.p.i. (ICP15). For images (A) to (F), arrows: inflammatory infiltrate; asterisk: muscle degeneration; dashed line: thickness of the circular smooth muscle layer. Bar: 50 µm (10×) A, B, C, D, E, and F; 20 µm (20×) insert F. (G) Clinical score of the histopathological aspects of the control and the infected acute and chronic phases groups. (H) For each animal, the thickness of the muscular layer value was calculated from the average of 10 images in H&E (10× objective) (n = 5, for each group). For (H), statistical analysis: two-way ANOVA and Student–Newman–Keuls. Control (○); Infected (●). For (H), the symbols (*) represent differences to the group (control vs infected) and the letters represent the difference in the time, regarding the same group. [a]Different from AP (ie, ICP3, ICP7, ICP12, and ICP15 were different from IAP). $P \leq 0.05$. Data presented as mean ± SD. (I) Macroscopic aspects of the megacolon of mice infected (ICP15) compared to control mice (CCP).

the colon (control and infected mice), at all time intervals studied. For each image (covering 316 629 μm^2), 3 measurements (μm) of the inner muscle layer thickness were obtained using the Image J 1.52 software (NIH, Bethesda, MD, USA). The inner muscle layer was defined by the boundaries of the submucosal layer and the outer muscle layer.[3] We expressed the data as mean ± SD. All the morphometric analyses were blinded.

Ex Vivo Organ Chamber Experiments

Preparation of circular muscle strips and isometric tension recordings

To perform ex vivo organ chamber experiments after the euthanasia, the colon was collected, separated from the mesentery, and washed in Krebs solution (in mM: 110.8 NaCl, 5.9 KCl, 25.0 $NaHCO_3$, 1.07 $MgSO_4$, 2.49 $CaCl_2$, 2.33 NaH_2PO_4, and 11.51 glucose, pH 7.4) to remove the fecal contents.[27] The colon was cut into rings (approximately 3 mm long) and 2 metal rods were pierced at the borders of the segments. In each experiment, 4 strips (obtained randomly from the distal and median portions) from the same specimen were simultaneously studied. One metal rod was fixed in the organ bath and the other rod was affixed to an isometric transducer (World Precision Instruments, Inc, Sarasota, FL, USA) connected to an amplifier (TBM4M; World Precision Instruments, Inc) and coupled to a computer equipped with an analog-to-digital converter board (Dataq Instruments, Akron, OH, USA). Preparations were placed in 10 mL organ baths filled with Krebs solution (37°C, bubbled with a mixture of 5% CO_2/95% O_2, pH 7.4). After mounting, segments were subjected to a resting tension of 0.5 g, over 1 hour to stabilize the preparation. After an equilibration period of 1 hour,[30] strips developed spontaneous phasic contractions. After the stabilization period, the preparations were challenged electrically or pharmacologically for contractility assays. This technical replicate was used to ensure the reliability of single values and prevent distortions caused by anatomic location.

Experimental design

The experiments included (1) the assessment of mechanical responses induced by the stimulation of enteric motor neurons (EMN)s by EFS, and (2) the study of contractile responses induced after drug exposure. Voltage rectangular pulses were applied by an electrical stimulator (Model SD9; Grass Technologies, Astro-Med, Inc, West Warwick, RI, USA). Control and infected colons were subjected to increasing electrical stimuli frequency: 0.5, 1, 5, 10, and 20 Hz.[31] Each stimulus was delivered by placing 2 platinum electrodes close to the segments. We have applied 10-second trains of pulses of 0.4 milliseconds duration at 1-40 Hz and 26 V (~100 mA) delivered to the platinum electrodes. Changes in tension were recorded simultaneously to electrical stimulation. The ON time was the same time used for stimulation (10 seconds). OFF time was immediately after ON time up to 1:30-2:00 minutes. ON contractions were evaluated during the 10 seconds stimulation and OFF contractions were evaluated after 10 seconds and up to 1:30-2:00 minutes. Finally, the stimulus used in our protocols resulted higher than usual since the response in Chagasic mice is very low. However, we tested the viability of all our preparations after the electrical stimulation, and all kept viable, as tested by KCl or ACh stimulation. Moreover, Barth et al[32] used 50 V, 20 pulses/second, to stimulate the intestine without tissue damage.[33] Simultaneously, ON and OFF-contraction waves were recorded through a synchronized transistor-transistor logic electrical signal Grass S88 and the Biopac system. ON-contractions waves were characterized as the contractile responses developed during the application of voltage pulses. OFF-contractions waves were characterized as the contractile responses developed immediately after the end of the stimulation protocol. The latency (time in seconds between the application of electrical stimuli and the beginning of the contractile response) of the ON- and OFF-contraction waves and the amplitude for the OFF-contraction waves (characterized by the peak of contraction in g/mg) were measured.

For pharmacological tests, the strips were exposed to muscarinic agonist acetylcholine (Ach; 10 μM; A6625; Sigma-Aldrich). The preparations were then washed and stabilized for 15 minutes followed by incubation with the NO synthase enzyme inhibitor (N^{ω}-nitro-L-arginine methyl ester [L-NAME] 300 μM; N5751; Sigma-Aldrich) for another 15 minutes. In the presence of L-NAME, the preparations were again stimulated with acetylcholine (ACh, 10 μM). The contractile response to the stimuli listed above was measured and expressed as amplitude (g/mg of dry tissue).

To evaluate the possible contraction induced neural component by acetylcholine, the protocols described below were used in the presence of tetrodotoxin or d-tubocurarine chloride. Tetrodotoxin (TTX; 100 nM; T8024; Sigma-Aldrich) was added to block the neuronal action potential by blocking voltage-dependent Na^+ channels. Thus, incubation with TTX excludes the participation of enteric innervation in the contractile response induced by ACh. To inhibit the activity of nicotinic receptors, we used d-tubocurarine chloride (50 μM; T-2379; Sigma-Aldrich). Atropine was used (1 μM; A0132; Sigma-Aldrich) to inhibit the activity of muscarinic receptors and assess whether the contractile effect of ACh is due

to direct stimulation of nicotinic receptors on intestinal smooth muscle. We evaluated the amplitudes related to the combined pharmacological stimuli described below: ACh + TTX + atropine; ACh + TTX + d-tubocurarine; ACh + TTX + L-NAME. To avoid possible intervening effects on the test results, the data of ex vivo contractility was plotted as the difference of contraction between the basal state and in response to ACh. After carrying out the experiments, the colons were carefully removed and left in an airy environment to allow complete tissue drying (48 hours), followed by weighting. To avoid variations in the data due to the difference in mass of the evaluated tissues, the contractility amplitude values (expressed in g) were normalized by the dry tissue mass (expressed in mg).[34]

Evaluation of cholinergic receptor expression in colon fragments by Western blot

The expressions of muscarinic acetylcholine receptor M3 subtype (mAChR M3; sc-9108; Santa Cruz Biotechnology, Santa Cruz, CA, USA; RRID: Addgene_114189) and acetylcholine receptor α7 subunit (AChRα7; sc-5544; Santa Cruz Biotechnology; RRID: AB_384861) receptors in the infected colon were evaluated and compared to the control. The colon tissue fragment was homogenized in a lysis buffer of (in mmol/L) 150 NaCl, 50 Tris HCl, 5 EDTA.2Na, and 1 $MgCl_2$ containing 1% Triton X-100 and 0.5% SDS plus protease inhibitors (SigmaFast; Sigma-Aldrich).[31] The lysate was centrifuged at 14 000 rpm for 20 minutes to separate the protein fraction. The amount of protein in the samples was determined by measuring the absorbance by spectrophotometry (260 nm in Nanodrop; ThermoScientific, Waltham, MA, USA). The samples were diluted in sample buffer (4 × 0.25 M tris HCl, pH 6.8, 3% Glycerol, 1% SDS, 0.6% beta-mercaptoethanol, 0.25% Bromophenol blue) and heated at 100ºC for 5 minutes.[31] For separation, 60 μg of protein was applied on 10% sodium dodecyl [lauryl] sulfate-polyacrylamide (SDS-PAGE) gel using the Mini-Protean Tetra Cell system (Biorad, Hercules, CA, USA). After the proteins were separated on the polyacrylamide gel (100 V; 90 minutes), they were transferred (100 V; 100 minutes) to a nitrocellulose membrane with a 0.45 μm pore (Millipore, Burlington, MA, USA). The membrane was first washed in distilled water and then placed for 1 hour in a blocking solution (3% albumin and 0.1% Tween-20, in Tris-buffered saline [TBS]). After blocking, the membrane was incubated overnight at 4ºC with the specific primary antibody diluted in blocking solution. The following primary antibodies were used: anti-mAChR M3 and anti-AChRα7. Then, the membrane was washed with TBS containing 0.3% Tween 20 (TBS-T) for 5 minutes (3 times) and incubated for 2 hours with secondary antibodies conjugated to Alexa Fluor 488 fluorescent probes (1:1000) diluted in 1% albumin in TBS-T. After the incubation period, the membrane was washed again in TBS-T for 5 minutes (3 times).[35] The bands were detected by a fluorescence reaction and their intensity was evaluated by densitometry analysis using the ImageJ 1.52 software.

Neurokinin 1 receptor, choline acetyltransferase, vasoactive intestinal polypeptide, and neuronal nitric oxide synthase detection by real-time reverse transcription–polymerase chain reaction

Colon samples were prepared for RNA extraction by adding 500 μL of RNA extraction reagent (15596; Trizol Reagent; Fisher Scientific, Hampton, NH, USA). After that, 100 μL of chloroform were added followed by homogenization for 15 seconds, incubation for 3 minutes on ice, and centrifugation at 12 000 g for 15 minutes at 4ºC. The supernatant was collected and isopropanol was added, with subsequent incubation on ice for 15 minutes and centrifugation at 12 000 g for 15 minutes at 4ºC. The pellet was washed with 75% chilled ethanol, followed by homogenization in the vortex and centrifugation at 7500 g for 5 minutes at 4ºC. The pellet was resuspended in 30 μL of RNase and DNase-free water and followed by a dry bath at 55ºC for 10 minutes. The quantification of the extracted RNA was performed using the Nanodrop equipment (Nano Vue Plus Spectrometer; GE Healthcare, Chicago, IL, USA) in ng.

Complementary DNA was obtained and real-time reverse transcription–polymerase chain reaction (RT-PCR) was performed as described previously using Real-Time PCR Detection System (CFX Manager version 3.1; Bio-Rad Laboratories, Inc, Hercules, CA, USA).[36] PCR amplifications were carried out using SYBR Green PCR Core Reagents Kit and performed as recommended by the manufacturer in a total volume of 20 μL containing 6 μL of cDNA. Each PCR amplification was performed in duplicate wells, using the following conditions: 2 minutes at 50°C and 10 minutes at 95°C, followed by a total of 45 two-temperature cycles (15 seconds at 95°C and 1 minute at 60°C) followed by a dissociation stage for detecting unspecific product formation. No unspecific PCR product was detected. Relative quantification was evaluated using $2^{-\Delta\Delta CT}$ using the uninfected groups as reference.[32] Primers (Applied Biosystems, Waltham, MA, USA) for the target genes are listed below: NK1-forward: GGTCTGACCGCAAAATCGAAC; NK1-reverse: AGAGCCTTTAACAGGGCCAC; ChAT-forward: AGGGCAGCCTCTCTGTATGA ChAT-reverse: ATCCTCGTTGGACGCCATTT; VIP-forward: GCAAGAT-

GTGGGACAACCTC VIP-reverse: CAGTCTGTTGCTGCTCATCC; nNOS-forward: ATGAAGTGACCAACCGCCTT and nNOS-reverse: AGCTGAAAACCTCATCTGTGTC. Data were normalized using glyceraldehyde-3-phosphate dehydrogenase (GAPDH)-forward: GACACCTTTGGCATTGTGG; GAPDH-reverse: ATGCAGGGATGATGTTCTG, amplified in the same assay plate.

Real-time polymerase chain reaction for parasite DNA

Tissue parasitism was evaluated in frozen samples submitted to the detection of parasite DNA by RT-PCR as described by Ricci et al.[3] Briefly, colon samples were prepared for DNA extraction by Promega Wizard Genomic DNA Purification kit, following the manufacturers' instructions. PCR reaction was performed in 10 μL containing 50 ng of genomic DNA (2 μL), 5 μL of SYBR Green PCR Mastermix (Applied Biosystems) and either 0.35 μM for *T. cruzi* DNA-specific primers or 0.35 μM of murine-specific TNFα primers and water. The primers for *T. cruzi* DNA (TCZ-F 5'-GCTCTTGCCCACAMGGGTGC-3', where M = A or C and TCZ R 5'-CCAAGCAGCGGATAGTTCAGG-3') amplify a 182-bp. Primers for murine TNFα (TNF-5241 5'-TCCCTCTCATCAGTTCTATGGCCCA-3' and TNF5411 5'-CAGCAAGCATCTATGCACTTAGACCCC-3') amplify a 170-bp product.[37]

Cycles of amplification were carried out in a 7500 Fast Real-Time PCR System (Applied Biosystems). Amplification was immediately followed by a melt program with an initial denaturation of 15 seconds at 95°C, cooling to 60°C for 1 minute and then a stepwise temperature increases of 0.3°C/second from 60°C to 95°C. Each 96-well reaction plate contained a standard curve and 2 negative controls. Standard curves were produced from a 10-fold DNA dilution of epimastigotes of *T. cruzi* Y strain and DNA from colon tissue of non-infected mouse, ranging from 1 × 106 to 1 parasites and equivalent/25 μg of tissue DNA. Negative controls consisted of a reaction with *T. cruzi*-specific or murine-specific primers without DNA and also with non-infected mouse tissue DNA. Each DNA sample was quantified in duplicate. The efficiencies of amplification were determined automatically by the 7500 Fast Real-Time PCR Software. Quantitative PCR showed amplification efficiencies > 90% and a regression coefficient (r^2) of 0.98.

Statistical Methods

Normalization for contractility experiments was performed to control the variations in the contractility amplitude values. Colon dry weight was used to normalize the records obtained in contractility experiments. The contractility amplitude values expressed in g were normalized by the colon dry weight in mg.

The Shapiro-Wilk test revealed that the parameters evaluated did not show a significant departure from a normal distribution. Two-way analysis of variance (ANOVA) was used to compare the thickness of the inner muscular layer, total, and colon transit time, amplitude and latency of contraction and expression of neurotransmitters between treatments (ie, control vs infected) and across time points (ie, AP, CP3, CP7, CP12, and CP15). Paired Student's *t* tests were used to compare motility in vivo assays with pyridostigmine treatment and muscarinic and nicotinic between groups (ie, control vs infected). In the presence of L-arginine analogs such as L-NAME, N^G-nitro-L-arginine modifies the basal contraction justifying the normalization.[31]

When a significant F value was found, we performed post hoc analyses according to the coefficient of variation (CV): Student–Newman–Keuls' tests (CV between 15-30%) or Duncan (CV > 30%). Statistical analyses were performed using the GraphPad Prism program (version 7.0) (GraphPad Software Inc., La Jolla, CA, USA). The α level was set at 0.05. Data are shown as mean ± SD.

Drugs

Isoflurane (BioChimico, Itatiaia, Brazil) was used for general inhalation anesthesia. Carmine red (Merck) stock solution was suspended in 0.5% methylcellulose (Merck). Pyridostigmine, ACh, TTX, L-NAME, atropine, and d-tubocurarine chloride were obtained from (Sigma-Aldrich), and dissolved in Krebs solution.

Results

Alongside the development of the murine megacolon, we evaluated the impairment of muscle contractility and its impact on colonic motility and investigated the molecular mechanisms involved in the impairment of neuronal, muscarinic, and nicotinic pathways.

Murine Chagasic Megacolon

Histopathological changes in infected animals were assessed during acute and various chronic time points. As described before, we analyzed the entire extension of the colon at 3, 7, 12, and 15 m.p.i.[29] Acute infection (IAP) was associated with increased inflammatory infiltration which presented a progressive attenuation or modification along the time paralleled to decreased tissue parasitism (Fig. 1A-F). From 7 m.p.i., the chronic inflammation persistent

with an associated was increased of the muscular layer by 12 and 15 m.p.i. (Fig. 1E and 1F).

The histopathological findings (Fig. 1G) show acute inflammation, cellular damage, and parasitism decreased over time, chronic inflammation persisted associated with increasing muscular wall thickness (Fig. 1H). There was macroscopic evidence of an increase in the length of the intestine (mega dolichocolon) in the infected mice by 15 m.p.i. compared to non-infected (Fig. 1I). Also, all animals used for the motility in vivo assays and ex vivo organ chamber experiments were positive for *T. cruzi* DNA. The average quantities of DNA detected by 25 μg of colon tissue were mean ± SD at acute phase (131 294.2000 ± 150 482.9000), which was significantly different than 232.5000 ± 259.8846, 329.1405 ± 388.3249, 271.8613 ± 338.2687, and 174.2698 ± 236.1740, respectively at 3 m.p.i., 7 m.p.i., 12 m.p.i., and 15 m.p.i.

Trypanosoma cruzi Infection Impairs Intestinal Motility In Vivo

Peristalsis was estimated by the colonic transit time and total transit time; thus, the longer the transit time, the lower intestinal motility. Colonic transit time increased in ICP15 compared to all other infected groups (ie, IAP, ICP3, ICP 7, and ICP12) indicating that colon motility decreased in 15 months of chronic infection (Fig. 2A).

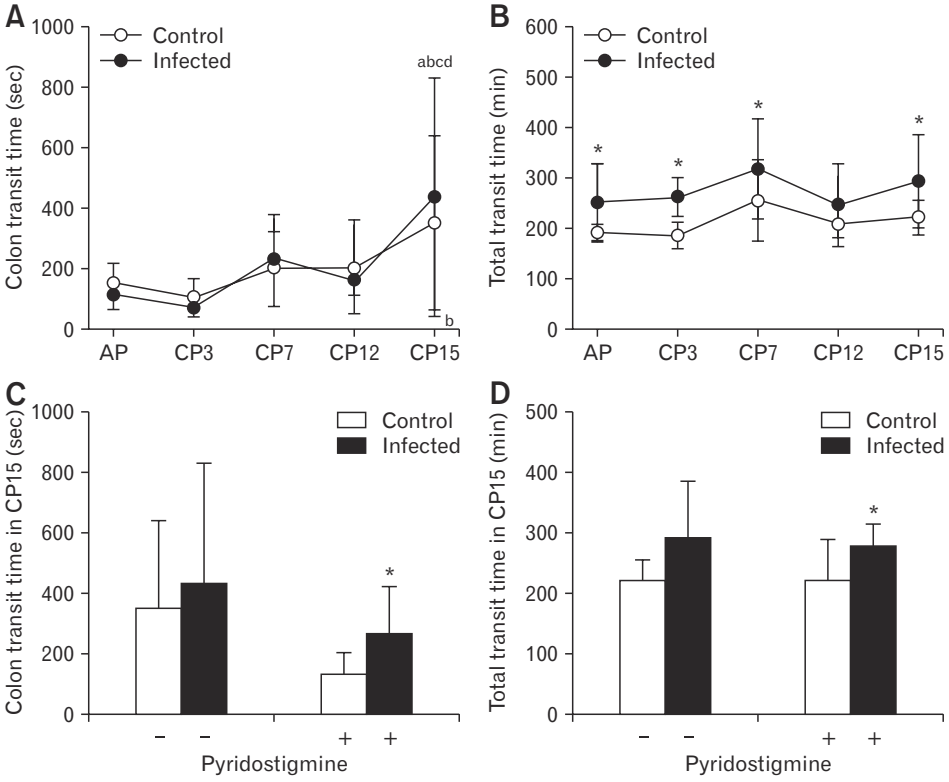

Figure 2. Colonic and total gastrointestinal (GI) tract motility are delayed throughout the experimental times. Control and infected groups were evaluated in the acute phase (AP; 11 days) and chronic phases (CP; 3, 7, 12, and 15 months post-infection [m.p.i.]) of *Trypanosoma cruzi* infection (A) Colonic transit time estimated by measuring the time required to release a glass bead. (B) Total transit time, estimated by measuring the time between carmine red orally administration and the time to excretion of red stools. n = 10 mice, except for infected acute phase (IAP) and infected chronic phase 3 m.p.i. (ICP3) groups, n = 16 and n = 15, respectively. For (A) and (B), statistical analysis: two-way ANOVA and Student–Newman–Keuls. Control (○); Infected (●). The symbols (*) represent differences in the relation to the group (control vs infected) and the letters (a, b, c, and d) represent the difference in the time, considering the same group. [a]Different from AP (ie, ICP15 was different from IAP). [b]Different from CP3 (ie, ICP15 was different from ICP3; CCP15 was different from CCP3). [c]Different from CP7 (ie, ICP15 was different from ICP7). [d]Different from CP12 (ie, ICP15 was different from ICP12). (C) Colonic transit time in 15 m.p.i. mice in the absence (–) or in the presence (+) of pyridostigmine. (D) The GI total transit time in 15 m.p.i mice in the absence (–) or in the presence (+) of pyridostigmine. n = 10, except for CCP 15 and ICP15 groups, n = 9 and n = 8, respectively. For (C) and (D), statistical analysis: Student's *t* tests. $P \leq 0.05$. Data presented as mean ± SD. The symbols (*) represent differences in the relation to the group (control vs infected).

The total transit time was higher to IAP, ICP3, ICP7, and ICP15 compared to respective non-infected controls. Altogether, our results indicate an intestinal impairment in the peristalsis, reducing whole intestinal motility.

At 15 m.p.i., we treated the animals with pyridostigmine, an inhibitor of acetylcholinesterase that increases the bioavailability of acetylcholine at the synaptic clefts. Regarding pyridostigmine-treated animals, the infected group presented increased colonic transit time compared to the control (Fig. 2C). Also, pyridostigmine administration induced a longer total transit time of the infected group (ICP15) in comparison to the control group (CCP15) (Fig. 2D).

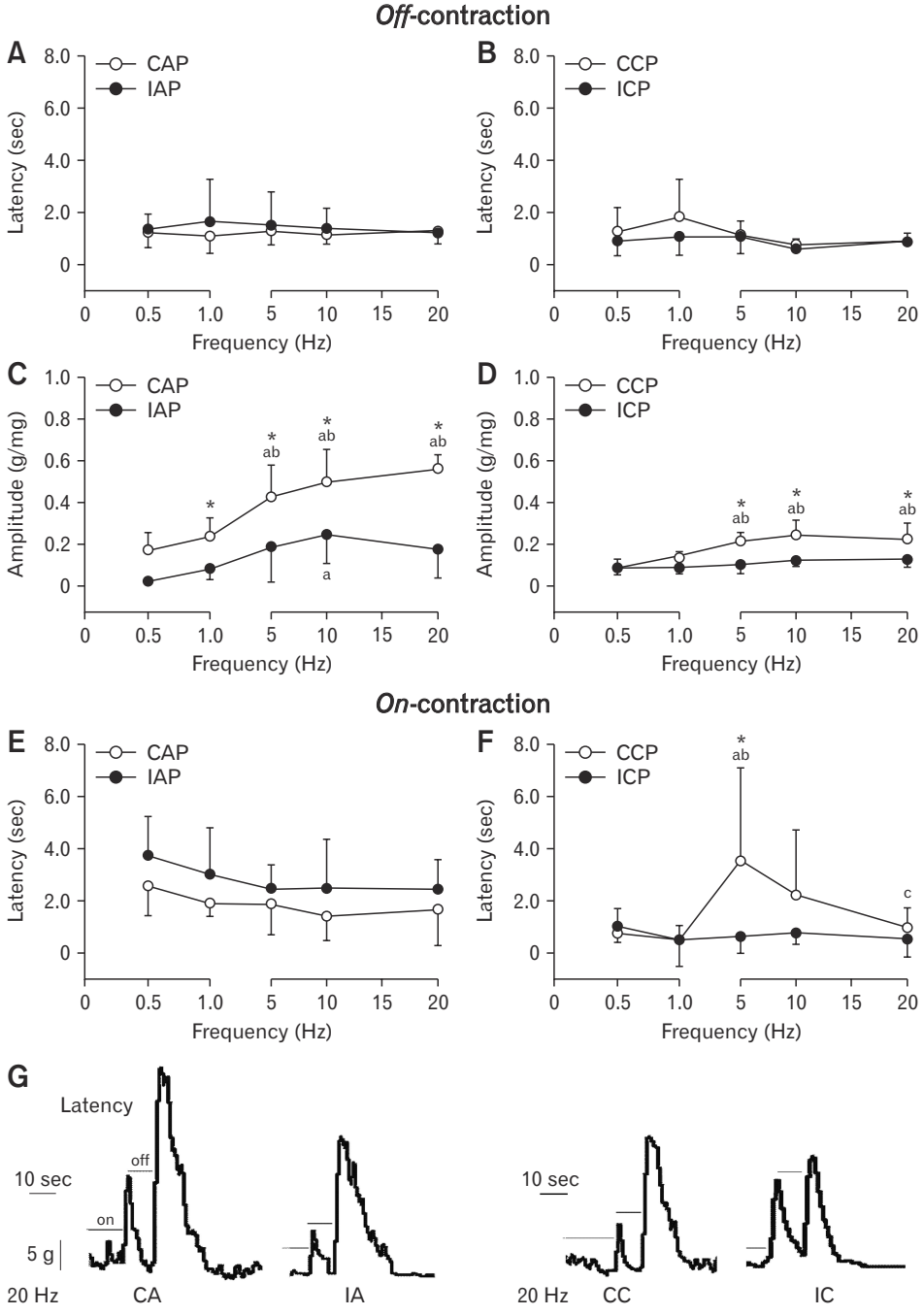

Figure 3. Electrophysiological responses (latency and amplitude of contractility) were obtained by stimulation of colon tissue circular strips. Control and infected groups were evaluated in the acute phase (AP; 11 days) and chronic phase (CP; 15 months post-infection [m.p.i.]) of *Trypanosoma cruzi* infection. Electrical stimuli of 0.5, 1, 5, 10, and 20 Hz were applied to colon tissue fragments in an organ bath system. (A and B) Latency in OFF-contractions. (C and D) Amplitude in OFF-contractions. (E and F) Latency in ON-contractions. n = 5, for each group. For (A) to (F), statistical analysis: two-way ANOVA and Duncan. Control (○); Infected (●). The symbols (*) represent differences in the relation to the group (control vs infected) and the letters (a, b, and c) represent the difference in the frequency, regarding the same group. [a]Different from 0.5 Hz. [b]Different from 1.0 Hz. [c]Different from 5.0 Hz. $P \leq 0.05$. Data presented as mean ± SD. (G) Schematic drawing indicating the ON- and the OFF-latencies and the highest peak amplitude of the off contraction. CAP, control acute phase; IAP, infected acute phase; CCP, control chronic phase; ICP, infected chronic phase.

Infection Decreases the Electrically-stimulated Elicited Contractile Responses

In our model, megacolon alterations include hypertrophy of the circular muscular layer, focal inflammatory reactions in the vicinity of the myenteric plexus and the muscular layer, and fibrosis of the myenteric plexus more pronounced at the distal portion of the colon confirming aspects described for the human disease.[38,39] Our sampling method was used to correlate anatomic pathology and functional data, avoiding result biases associated with inadequate sample location.

To better evaluate the muscle function of infected intestines, we stimulated strips of the colon with low-frequency electrical waves. As expected, the colon responded with OFF-contractions, and was used to compare the intestinal muscle contractility between groups. Amplitude and latency of the contractile response were assessed by increasing stimulation frequency above 5 Hz (Fig. 3).

There were no differences in the latency of OFF-contraction between CAP and IAP nor between CCP and ICP (Fig. 3A and 3B). Moreover, increasing stimuli intensity did not change the latency of off-contractions in both CAP and CCP groups (Fig. 3A and 3B). However, increasing stimuli induced a higher amplitude of contractions in CAP compared to the CCP group (Fig. 3C and 3D and Supplementary Figure), a mechanism possibly associated with aging. Importantly, the CCP group poorly responded to the increase in electrical stimulation (Fig. 3D). Both infected groups (IAP and ICP) presented a lower response compared to their respective controls, especially after 5 Hz stimulation (Fig. 3C and 3D).

ON-contractions latency was higher in infected mice during the acute phase (IAP), compared to the respective control group (CAP) (Fig. 3E). However, there were no differences under in-

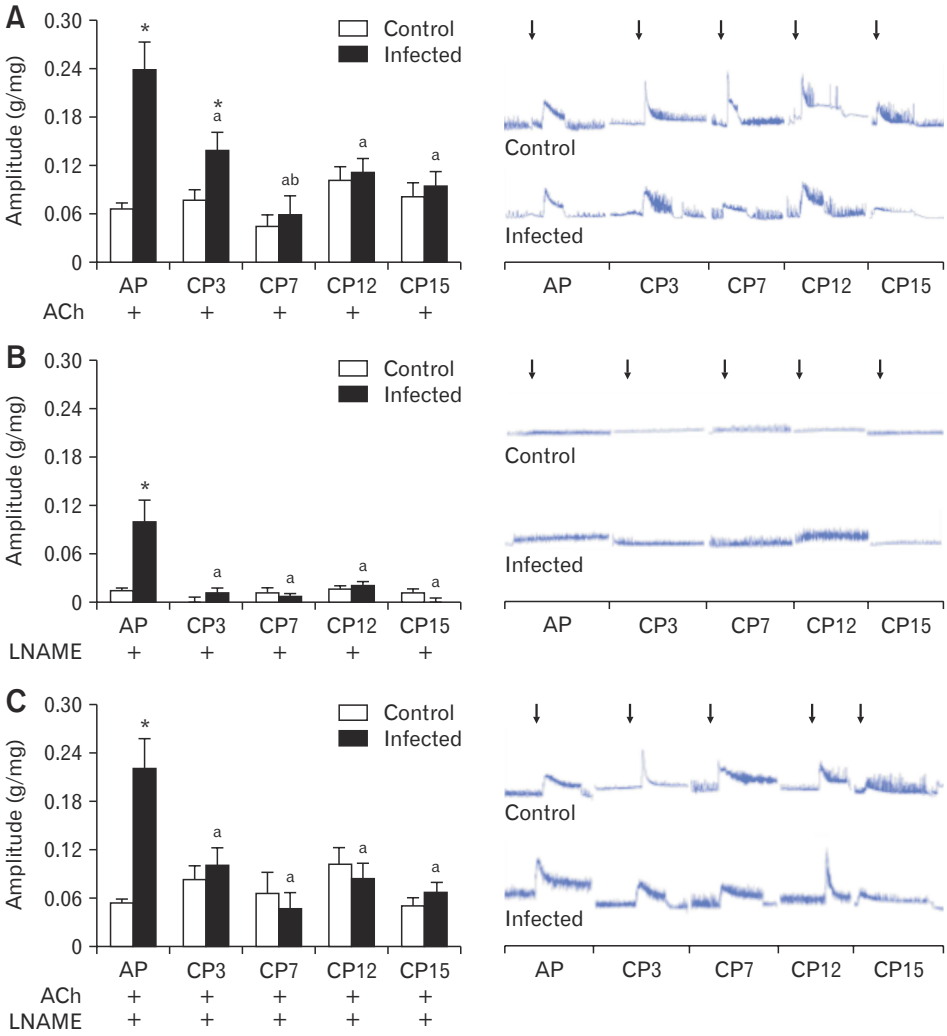

Figure 4. Electrophysiological responses (amplitude of contractility) were obtained by stimulation of colon tissue circular strips in the presence of acetylcholine (ACh), L-NAME, and L-NAME + ACh. Control and infected groups were evaluated in the acute phase (AP) [11 days] and chronic phase (CP) [3, 7, 12, and 15 months post-infection (m.p.i)] of *Trypanosoma cruzi* infection. To the colon tissue fragments in an organ bath system was added (A) Acetylcholine (ACh), followed by inhibition with (B) N^{ω}-nitro-L-arginine methyl ester (L-NAME) and then (C) ACh. Statistical analysis: two-way ANOVA and Student–Newman–Keuls. n = 5, for each group, except for control CP12, CP15, and infected CP3 and CP12, n = 4. Control (○); Infected (●). The symbols (*) represent differences in the relation to the group (control vs infected) and the letters (a, b) represent the difference in the frequency, regarding the same group. [a]Different from AP. [b]Different from CP3. $P \leq 0.05$. Data presented as mean ± SD. In the schematic drawing next to the graphs, the arrows indicate the ACh time point administration.

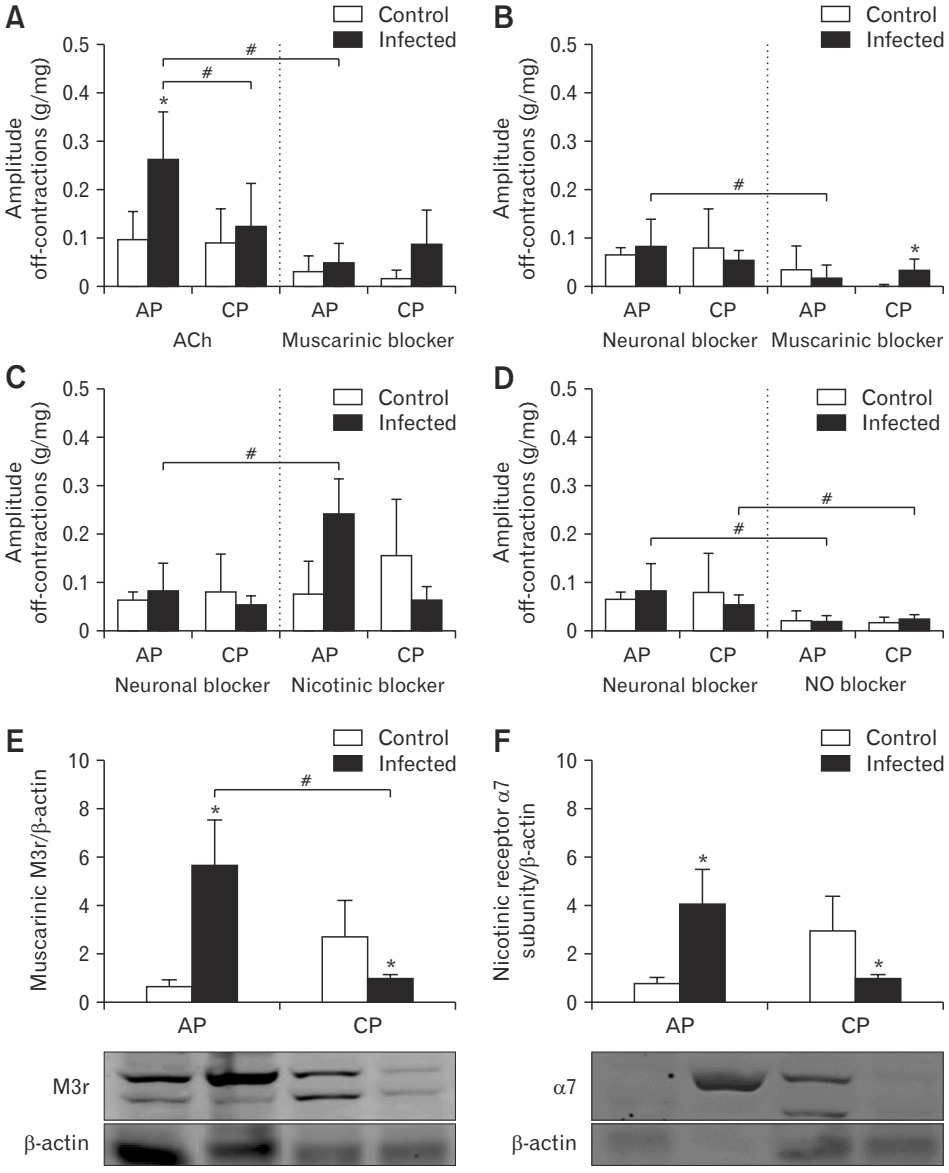

Figure 5. Electrophysiological responses (amplitude of contractility) obtained by stimulation of colon tissue circular strips with inhibition of muscarinic, neural, and nicotinic pathways; and expression of nicotinic and muscarinic receptors. Control and infected groups were evaluated in the acute phase (AP; 11 days) and chronic phase (CP; 15 months post-infection [m.p.i]) of *Trypanosoma cruzi*. Colon fragments were incubated with acetylcholine (ACh; 10 μM), atropine (muscarinic blocker; 1 μM), tetrodotoxin (neuronal blocker; 100nM), d-tubocurarine chloride (nicotinic blocker; 50 μM) methyl ester of N (ω) -nitro-L-arginine (L-NAME, nitric oxide [NO] blocker; 300 μM). (A) ACh + Muscarinic receptor block. (B) Neural block + Muscarinic receptor block. (C) Neural block + Nicotinic receptor block. (D) Neural block + NO block. n = 4 for contraction amplitude. (E and F) The colon tissue expression of proteins of muscarinic type 3 receptor (anti-M3r) and nicotinic alpha 7 receptor (anti-α-7) of the control and the infected groups of the AP and the CP15 m.p.i. were measured by Western blot. β-actin was used as a control protein. n = 5 for Western blot analysis. Statistical analysis: Student's *t* tests. Control (○); Infected (●). The symbols (*) represent differences between the groups (control vs infected). The symbols (#) represent differences between the groups infected. $P \leq 0.05$. Data presented as mean ± SD.

creasing the frequency of electrical stimulation in control compared to infected (Fig. 3E). On the other hand, in the chronically infected mice (15 m.p.i.) the latency period was significantly shorter compared to their paired control at the 5 Hz frequency (Fig. 3F). See the graphic representation of the patterns of electric field stimulation in Figure 3G.

Smooth Muscle Hyperresponsivity to Acetylcholine and Involvement of Nitric Oxide Synthase in the Acute Phase

ACh is one of the main neurotransmitters that induce intestinal muscle activity[13] while NO is associated with muscle relaxation. We tested the intestinal contractility response upon exposure to ACh. Ach significantly increased the amplitude of contractions in the acute-phase infected group (IAP) and infected 3-month chronic phase (CP3) compared to the respective controls (Fig. 4A). Interestingly, there were no differences in the amplitude of ACh-induced contractions between infected and control groups after 7, 12, or 15 months (Fig. 4A).

NOS inhibition with L-NAME increased the amplitude of contractions only in the acute-phase infected group (IAP), compared to control (Fig. 4B). However, pre-incubation with L-NAME previously to ACh stimulation did not change the effects of ACh stimulation in acutely infected mice but abolished the increase in contraction in CCP3 infected mice, compared to control (Fig. 4C).

Neuronal, Muscarinic, and Nicotinic Responses to Acetylcholine in the Acute and Chronic Stage of Infection

To better investigate the pathways involved in intestinal muscle activity during *T. cruzi* infection, we used ACh receptors (AChR) blockers targeting nicotinic and muscarinic receptors. The amplitude of ACh-induced contraction did not differ in acute and

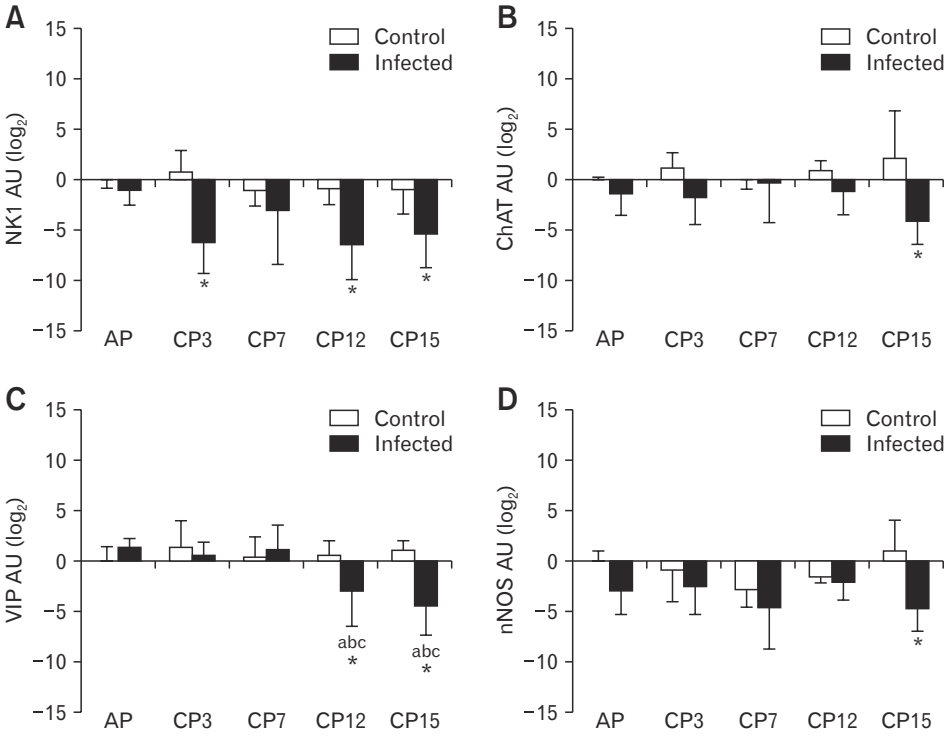

Figure 6. Expression of excitatory (neurokinin 1 [NK1] and choline-acetyltransferase [ChAT]), and inhibitory (vasoactive intestinal polypeptide [VIP] and neuronal nitric oxide synthase [nNOS]) receptors in colon tissue. Control and the infected group were evaluated in the acute phase (AP; 11 days) and chronic phase (CP; 15 months post-infection [m.p.i.]) of *Trypanosoma cruzi* infection. The colon tissue gene expression of the neurotransmitter receptors was measured by the real-time polymerase chain reaction assay. (A) NK1, (B) ChAT, (C) VIP, and (D) nNOS. Statistical analysis: two-way ANOVA and Student–Newman–Keuls. n = 5, except for control AP, CP3, CP7, CP12, and infected CP3, n = 4; and for control CP15, n = 3. Control (○); Infected (●). The symbols (*) represent differences in the relation to the group (control vs infected) and letters (a, b, and c) represent the difference in the time, regarding the same group. [a]Different from AP. [b]Different from CP3. [c]Different from CP7. $P \leq 0.05$. Data presented as mean ± SD.

chronic controls (Fig. 5). ACh administration resulted in a higher amplitude of contraction only in the acute phase of infection (IAP), compared to the control (CAP) (Fig. 5A). Consequently, ICP15 presented a lower amplitude of contraction than IAP.

Atropine, a muscarinic antagonist, significantly decreased the amplitude of contraction previously induced by ACh in the IAP, suggesting a role of smooth muscle muscarinic receptors in increased contraction during the acute phase of infection (Fig. 5A). However, the residual response to ACh under atropine treatment suggested the involvement of smooth muscle nicotinic receptors. To exclude the possible release of neuronal ACh by nicotinic receptors stimulation, we used the neuronal blocker TTX. TTX did not induce any difference in contractility between control and infected groups (Fig. 5B-D). In the presence of TTX, the addition of atropine resulted in decreased amplitude in the IAP group compared to the neural block only. Muscarinic receptor antagonism in neuronal-blocked preparations with TTX abolished the contraction in CCP15 but not in ICP15, suggesting the involvement of smooth muscle nicotinic receptors during the chronic phase of infection (Fig. 5B). Nicotinic receptor antagonism with d-tubocurarine increased the contraction in IAP, suggesting downregulation of nicotinic receptors in the smooth muscle (Fig. 5C).

NOS inhibition in neuronal-blocked preparations reduced the amplitude of contractions but without any difference between the groups (Fig. 5D).

Expression of Muscarinic Type 3 Receptors and Nicotinic Alpha 7 Subunits of Nicotinic Receptors in Animals in the Acute and Chronic Stages of Infection

We investigated if differences observed in AChR activities were associated with protein regulation. So, we investigated the protein content of AChR by Western blot in the intestines. For both the M3r and α-7 subunits of nicotinic receptors (Fig. 5E and 5F), IAP animals presented a higher expression of receptors compared to their controls (CAP). Conversely, animals in the chronic phase of infection (ICP15) showed a reduction in both receptors compared to their respective control groups (CCP15). Animals of ICP15 showed a lower expression in these receptors (M3r and α-7 subunits of nicotinic receptors) compared to IAP.

Expression of mRNA for Excitatory and Inhibitory Neurotransmitters

We also evaluated the expression of the receptor NK1, which showed a significant reduction in the ICP3, ICP12, and ICP15 compared to their controls (Fig. 6A). The expression of the enzyme choline acetyltransferase (ChAT) was significantly lower in ICP15 compared to CCP15 (Fig. 6B).

There was a significant decrease in the mRNA expression for VIP in ICP12 and ICP15 groups compared to their controls. VIP mRNA expression reduced over time. ICP12 and ICP15 differ from IAP, and ICP15 also differs from ICP3 and ICP7 (Fig. 6C). For the nNOS, ICP15 showed a significant decrease in mRNA enzyme expression compared to their respective controls (Fig. 6D).

Discussion

The present study is the first to report patterns of stimulation and latency in a murine model of Chagasic megacolon. Our group and others previously described intestinal histopathological changes in the acute phase of *T. cruzi* infection.[2,6,40-42] Our recently described model induced the chronic phase of Chagasic disease in all mice infected with Y *T. cruzi* strain that survives by administering a single oral dose of benznidazole (500 mg/kg) at 11 d.p.i.[21] This treatment scheme prevents the acute death of around 50% of animals and guarantees that the circulating parasites reach the intestinal wall and trigger the local pathology.[3,21] At the acute phase, all animals presented colonic inflammation associated with parasitism. We confirmed that 20% to 30% percent of treated animals that reached the chronic phase of the disease (15 m.p.i.) presented progressive intestinal and ENS structural changes, associated with the persistence of chronic inflammation and smooth muscle hypertrophy reproducing the natural history of Chagas disease.[3,21] The treated surviving animals were followed through the chronic phase to study the inflammation, parasitism ganglionic neuronal damage, intramuscular denervation, and phenotype changes of intestinal *muscularis propria* denervation (smooth muscle hypertrophy) associated with megacolon development. Ricci et al,[3] also confirmed the persistence of parasites by immunolabelling with antibody anti-*T. cruzi* by 15 m.p.i. In addition, all animals included in the in vivo and in vitro assays here reported tested positive by quantitative RT-PCR for parasite DNA.

In this follow-up study, we confirmed the intense parasitism and inflammation in the acute phase that was followed by progressive colon wall thickening, which becomes significantly evident from 7 m.p.i. (Fig. 1H). Although the intensity of inflammation decreased from acute towards the chronic phase of infection, it persisted along with the development of Chagasic megacolon. The Chagasic megacolon is much associated with intestinal motility dysfunction. However, the origin, regulation, and timeline of intestinal wall con-

tractions are not yet fully understood,[43] limiting the comprehension of intrinsic mechanism(s).

The time required to eject the bead was measured as an estimate of colonic motility. Our in vivo studies showed increased colon transit time in the infected chronic group (ICP15) compared to all the infected groups (IAP, ICP3, ICP7, and ICP12). Chronically infected animals showed a progressive impairment of colonic motility compared to their controls (Fig. 2A). So the bead propulsion test resulted in a delayed bead propulsion time, as an estimate of uncoordinated motor activity of distal colon including the impaired relaxation of the anal sphincter (the distal 1 mm of the colon), which also can be identified in some patients with Chagas disease.[2,26,44]

The thickness of the inner muscular layer and the electrophysiological responses were systematically studied only in the colon, with significant functional impairment detected at 15 m.p.i. comparatively to earlier times.

The total GI transit time of the red dye indicates the function of the entire GI tract: small intestine and colon (Fig. 2B). Indeed, the total transit time indicated motility impairment from the early time points (acute phase), probably indicating that the small intestine is also affected by the infection (inflammation, edema, and parasitism) contributing to the intestinal motility disorder. Due to methodological limitations, we did not study systematically the small intestine by histology to make direct correlations. Total motility was more sensitive to detect early dysfunction, probably because the entire extension of the small intestine was evaluated in contrast with the small length of the distal colon (2-3 cm) assessed by colonic motility.

Both the colonic and total motility with pyridostigmine was not improved by increasing the availability of ACh to the infected animals, which kept presenting decreased motility parameters (significantly increased colonic and total motility time at IAP15) compared to their controls (Fig. 2C and 2D), and corroborating our previous impression of progressive structural impairment of the intestine from 7 m.p.i.[3]

One of the limitations of this work is the difficulty of performing structural and correlated functional analyzes in the various intervals between 11 d.p.i and 15 m.p.i. We did not perform the pyridostigmine test before 15 m.p.i, but data from our previous work using the same model indicate that the onset of structural changes occurs from 7 m.p.i. with increasing colonic wall thickness, and denervation from 12 m.p.i.[3] Herein, functional repercussions were studied at 15 m.p.i. These data indicate that at later time points there is structural and definitive damage to the enteric circuits involving the ACh, indicating that therapeutic intervention must be introduced earlier than the functional impairment is installed.

The organ chamber experiments may not reproduce the same pattern of contractions in vivo, but it is a good tool to compare the dynamics in the presence of the intervention (such as the *T. cruzi* long-term infection). In our experiments, we removed all the external modulation of colonic contractilities such as the central nervous system and possible humoral factors such as circulating catecholamines and other peptides and hormones. Even though, a few works showed the amplitude of in vivo contractions similar to our findings (lower than 0.5 g or 5 mN).[45,46]

The circular strips of the human colon commonly develop 2 distinct patterns of contractile responses of neural origin under EFS stimulation in ex vivo experiments: (1) a phasic contraction, which begins during EFS (so-called ON-contractions) or (2) a phasic contraction, which appears after EFS (OFF-contractions). We observed the same pattern of contraction in our model. Excitatory stimulation in the EMNs is related to the amplitude of EFS-induced ON- and OFF-contractions, which release ACh and tachykinins, mainly acting, respectively, on muscarinic and NK1/NK2 receptors, located on smooth muscle cells.[31,47,48]

In the infected chronic group, the amplitude did not increase with the increase of the stimulus frequency. Notice that the CCP group also did not respond to the increased stimulus. Several authors have previously described the cholinergic excitatory component of contraction in humans.[12,49,50] OFF-contractions latency did not change significantly between infected and control groups both at the acute and chronic phase (Fig. 3A and 3B). Also, we observed that the amplitude of contractile responses (Fig. 3C and 3D) to the electrical stimulus (OFF-contractions) in the infected groups of both acute and chronic phases was decreased in comparison to their controls.

ON-contraction latencies in the IAP group were increased in comparison to the CAP (Fig. 3E and 3F). Although not significantly, this could be related to edema and interstitial infiltration of the acutely inflamed wall. ON-contractions are practically abolished through the addition of atropine and tachykinin receptor antagonists.[51] The amplitude of ON-contractions was not measured in this work.

We analyzed the OFF-contraction amplitude under diverse modalities of intervention (Fig. 4). Acute infection caused hyperresponsiveness to ACh on colonic musculature which was probably associated with inflammatory-induced necrosis, collagen deposition, and disorganization, predominantly, of the circular smooth muscle layer. As a diffuse inflammatory process in the acute phase becomes more focal and gradual over time, with the development of muscular layer hypertrophy, there was a progressive reduction of muscle

hyper-responsiveness between 3 m.p.i. and 15 m.p.i.; however, the assays did not detect differences when comparing infected with control groups.

To evaluate if the intense and diffuse inflammatory infiltrate could be regulating the contractile response to ACh, we analyzed the role of NO produced in response to infection and the constitutive nNOS-derived NO. NO is an important neurotransmitter and mediator of the acute inflammatory process, participating actively in the defense process against pathogens. We used pharmacological tools to assess the contractile response pattern to ACh in colon fragments pre-incubated with NOS inhibitor and observed an increase in the basal contractile responses. However, contractile responses to ACh do not differ when comparing control vs infected mice from 3 m.p.i. after inhibition of NOS, indicating that the probable source of NO was blocked during the acute inflammation.[40] These data corroborate with the literature demonstrating that increase in NO production is directly associated with a reduction in smooth muscle contractility in various inflammatory bowel conditions such as inflammatory colitis and Chron's disease.[52,53] Although not addressed in this study, the calcium-activated K channels such as ATP or a related purine may have participated in the inhibitory component of EMNs.[54,55]

The production of excitatory and inhibitory neurotransmitters is of great importance for the balance of intestinal function. The studies performed with individuals and animals models presenting megacolon have shown that neuronal NO is preserved[15,56] and that, there is evidence of ACh loss.[15] Based on the importance of the cholinergic system in the control of colonic contractility, we evaluated the effect of peripheral cholinesterase inhibition by using pyridostigmine (reversible inhibitor). When animals orally received pyridostigmine, we observed a significant increase in colonic transit time in the ICP15 compared to their controls. The infection reduces the sensitivity to ACh since the increased bioavailability of ACh resulted in reduced colonic motility for infected animals when compared to controls. Altogether our in vivo and ex-vivo assays suggest a possible downregulation of the cholinergic system so explaining the increased colonic transit time present in CD.

At the chronic phase (Fig. 5B), the amplitude of contractile waves in control mice was almost zero in presence of TTX and atropine, indicating that the observed basal contractions are mostly induced by muscarinic receptors under ACh activation in the musculature. Fifteen months post-infection, mice exhibited increased amplitude when compared to their controls which indicates possible pathways other than muscarinic receptor-dependent to control contraction in infected intestinal smooth muscle. Although not yet studied in Chagasic megacolon, molecular and functional plasticity of the GI gamma-aminobutyric acid type A receptor system was implicated in the age-induced colonic inflammation associated with healthy aging.[57] A reduction in the sensibility to ACh indicated by our data with pyridostigmine could also be associated with decreased expression of M3 and α-7 receptors in chronically infected tissues when compared to controls. In this line, the increase in the amplitude of contraction in ICP15 could be explained by the loss of intramuscular fibers, observed histologically in the infected mice in the chronic phase.[21] Altogether, our data indicate some degree of plasticity of the excitatory pathway along with the long-term infection. Smooth muscle cells hyperplasia and hypertrophy and the plasticity of smooth muscle affecting force production were demonstrated in the inflamed intestine,[58,59] however, the modulation of neurotransmitters and their receptors were not investigated. Our results also point that acute infection also alters the pathways of the excitatory motor reflex, including higher expression of subunits of ACh receptors. However, we need more tests to fully characterizing electrophysiological remodeling in the experimental and human colons. The amplitude of contraction was probably affected by atropine leading to (1) changes in the smooth muscle cell´s basal tone, (2) excitability of interstitial cells of Cajal, or even (3) inhibition of neurotransmitter release by EMNs through action potential-independent mechanisms.[28]

Muscarinic antagonism with atropine reduced but did not abolish contractile responses to ACh in both control and infected mice. Based on these data, we investigated the possible activation of nicotinic receptors in enteric neurons. Simultaneous neuronal blockade and atropine incubation reduced ACh-induced contraction in acutely infected mice, abolished the contraction in control of chronic mice, and did not change the contraction in chronically infected mice. These data support the hypothesis that nicotinic receptors could be physiologically expressed in colonic smooth muscle and could be modulated by aging and by infection.[60-64] Surprisingly, the use of the nicotinic receptor's antagonist increased ACh-induced contraction in the neuronal blocked colon. This data suggested that nicotinic receptors could lead to colonic smooth muscle relaxation and could be down-regulated during the chronic phase of Chagas disease. This hypothesis is also supported by Aulí and collaborators[31] in 2008, which showed a relaxant effect of nicotinic receptors in the colon. On the other hand, we also tested the possible modulatory effect of NO on ACh-induced contraction in the colon in CD. Our data suggested that neuronal NO could down-regulate the contraction in the acute phase but not in the chronic phase. In the chronic phase, despite the reduction of contraction after the

neuronal blockade and L-NAME incubation, there were no differences between control and infected groups. This data reinforces that nNOS is not the only neurotransmitter that could be involved in NO production in the colon during the development of CD.

The expression pattern of NK1, ChAT, VIP, and nNOS was examined along with the development of Chagasic megacolon. We detected a reduction in NK1 expression throughout time, which resulted in differences against the control groups at 3 and 7 months of infection, suggesting that excitatory mechanisms regulating colonic contractions in Chagasic megacolon may be impaired. The expression of ChAT, an indirect indicator of cholinergic activity, decreased in the ICP15 group compared to its non-infected control and also corroborates a role for cholinergic dysfunction in our model. VIP expression was also decreased by 15 m.p.i. compared to controls. Also, the infected animals presented a progressive reduction of VIP expression along the course of the disease. nNOS expression decreased by 15 m.p.i. compared to controls, reflecting possible damage or modification of the nitrergic system, even at the submucosal enteric plexus.[65] That contrasts with our finding of a relative increase of nNOS in Chagasic megacolon by immunohistochemistry myenteric ganglia,[56] which could also indicate that the preserved neurons at myenteric plexus at 15 m.p.i. changed its phenotype to inhibitory neurons.

In conclusion, our results described a colonic-derived impairment in the peristalsis associated with acute inflammation in the acute phase of CD and damage to EMNs and *muscularis propria* at chronic phases of infection. In this study, GI rhythmicity was affected in a murine model of Chagasic megacolon involving the lack of response of infected chronic animals related to changes in the cholinergic and SP components of excitatory response modified by the installation of the megacolon. The model will be valuable to the further characterization of the ENS impairment mechanisms of intestinal Chagas' disease with an emphasis on cholinergic dysfunction as a pathogenic mechanism.

Supplementary Material

Note: To access the supplementary figure mentioned in this article, visit the online version of *Journal of Neurogastroenterology and Motility* at http://www.jnmjournal.org/, and at https://doi.org/10.5056/jnm21074.

Financial support: This study was supported by CNPq (311976/2021-2) Fundação de Amparo à Pesquisa do Estado de Minas Gerais (FAPEMIG) (CDS-PPM 000304/16, PRONEX 305952/2017, PPM 00304-16, CBB-APQ-01419-14, APQ-00921-18) and by CAPES/Brazil (PhD and Post-Doctoral fellowships).

Conflicts of interest: None.

Author contributions: Mayra F Ricci: experimental design, experimental procedures, and manuscript preparation; Samantha R Béla: experimental procedures; Joana L Barbosa: manuscript preparation; Michele M Moraes: manuscript preparation; Ana L Mazzeti: experimental procedures; Maria T Bahia: experimental design and manuscript preparation; Laila S Horta: experimental procedures; Helton da C Santiago: experimental design and manuscript preparation; Jader S Cruz: manuscript preparation; Luciano dos S A Capettini: experimental design and manuscript preparation; and Rosa M E Arantes: experimental design, experimental procedures, and manuscript preparation. All authors approved the final version of the manuscript.

References

1. Koberle F. [Change disease: a disease of the peripheral autonomic nervous system.] Wien Klin Wochenschr 1956;68:333-339. [German]
2. da Silveira AB, Lemos EM, Adad SJ, Correa-Oliveira R, Furness JB, D'Avila Reis D. Megacolon in chagas disease: a study of inflammatory cells, enteric nerves, and glial cells. Hum Pathol 2007;38:1256-1264.
3. Ricci MF, Béla SR, Moraes MM, et al. Neuronal parasitism, early myenteric neurons depopulation and continuous axonal networking damage as underlying mechanisms of the experimental intestinal chagas' disease. Front Cell Infect Microbiol 2020;10:583899.
4. Lopes ER, Rocha A, Meneses AC, et al. [Prevalence of visceromegalies in necropsies carried out in Triângulo Mineiro from 1954 to 1988.] Rev Soc Bras Med Trop 1988;22:211-215. [Portuguese]
5. Bern C, Montgomery SP, Herwaldt BL, et al. Evaluation and treatment of chagas disease in the United States: a systematic review. JAMA 2007;298:2171-2181.
6. Meneghelli UG. chagas' disease: a model of denervation in the study of digestive tract motility. Braz J Med Biol Res 1985;18:255-264.
7. De Oliveira RB, Troncon LE, Dantas RO, Meneghelli UG. Gastrointestinal manifestations of chagas' disease. Am J Gastroenterol 1998;93:884-889.
8. Salvador F, Mego M, Sánchez-Montalvá A, et al. Assessment of rectocolonic morphology and function in patients with chagas disease in Barcelona (Spain). Am J Trop Med Hyg 2015;92:898-902.
9. Meneghelli UG, de Godoy RA, Macedo JF, de Oliveira RB, Troncon LE, Dantas RO. Basal motility of dilated and non-dilated sigmoid colon and rectum in chagas' disease. Arq Gastroenterol 1982;19:127-132.
10. Adad SJ, Cançado CG, Etchebehere RM, et al. Neuron count reevaluation in the myenteric plexus of Chagasic megacolon after morphometric

neuron analysis. Virchows Arch 2001;438:254-258.
11. Cavenaghi S, Felicio OC, Ronchi LS, Cunrath GS, Melo MM, Netinho JG. Prevalence of rectoanal inhibitory reflex in Chagasic megacolon. Arq Gastroenterol 2008;45:128-131.
12. Hinds NM, Ullrich K, Smid SD. Cannabinoid 1 (CB1) receptors coupled to cholinergic motorneurones inhibit neurogenic circular muscle contractility in the human colon. Br J Pharmacol 2006;148:191-199.
13. Bornstein JC, Costa M, Grider JR. Enteric motor and interneuronal circuits controlling motility. Neurogastroenterol Motil 2004;16(suppl 1):34-38.
14. Jabari S, da Silveira AB, de Oliveira EC, Quint K, Neuhuber W, Brehmer A. Preponderance of inhibitory versus excitatory intramuscular nerve fibres in human Chagasic megacolon. Int J Colorectal Dis 2012;27:1181-1191.
15. Jabari S, da Silveira ABM, de Oliveira EC, et al. Partial, selective survival of nitrergic neurons in Chagasic megacolon. Histochem Cell Biol 2011;135:47-57.
16. Dickson EJ, Spencer NJ, Hennig GW, et al. An enteric occult reflex underlies accommodation and slow transit in the distal large bowel. Gastroenterology 2007;132:1912-1924.
17. Costa M, Brookes S. Architecture of enteric neural circuits involved in intestinal motility. Eur Rev Med Pharmacol Sci 2008;12(suppl 1):3-19.
18. Furness JB, Callaghan BP, Rivera LR, Cho HJ. The enteric nervous system and gastrointestinal innervation: integrated local and central control. Adv Exp Med Biol 2014;817:39-71.
19. Spencer NJ, Hu H. Enteric nervous system: sensory transduction, neural circuits and gastrointestinal motility. Nat Rev Gastroenterol Hepatol 2020;17:338-351.
20. Tata AM, Velluto L, D'Angelo C, Reale M. Cholinergic system dysfunction and neurodegenerative diseases: cause or effect? CNS Neurol Disord Drug Targets 2014;13:1294-1303.
21. Campos CF, Cangussú SD, Duz ALC, et al. Correction: enteric neuronal damage, intramuscular denervation and smooth muscle phenotype changes as mechanisms of Chagasic megacolon: evidence from a long-term murine model of *Tripanosoma cruzi* infection. PLoS One 2016;11:e0153038.
22. Bafutto M, Luquetti AO, Gabriel Neto S, Penhavel FAS, Oliveira EC. Constipation is related to small bowel disturbance rather than colonic enlargement in acquired Chagasic megacolon. Gastroenterology Res 2017;10:213-217.
23. Kilkenny C, Browne W, Cuthill IC, Emerson M, Altman DG; NC3Rs Reporting Guidelines Working Group. Animal research: reporting *in vivo* experiments: the ARRIVE guidelines. Br J Pharmacol 2010;160:1577-1579.
24. McGrath JC, McLachlan EM, Zeller R. Transparency in research involving animals: the basel declaration and new principles for reporting research in BJP manuscripts. Br J Pharmacol 2015;172:2427-2432.
25. Brener Z. Therapeutic activity and criterion of cure on mice experimentally infected with *Trypanosoma cruzi*. Rev Inst Med Trop Sao Paulo. 1962;4:389-396.
26. Lin CY, Zhang M, Huang T, et al. Spexin enhances bowel movement through activating L-type voltage-dependent calcium channel via galanin receptor 2 in mice. Sci Rep 2015;5:12095.
27. Avetisyan M, Wang H, Schill EM, et al. Hepatocyte growth factor and MET support mouse enteric nervous system development, the peristaltic response, and intestinal epithelial proliferation in response to injury. J Neurosci 2015;35:11543-11558.
28. Fichna J, Schicho R, Andrews CN, et al. Salvinorin A inhibits colonic transit and neurogenic ion transport in mice by activating kappa-opioid and cannabinoid receptors. Neurogastroenterol Motil 2009;21:1326-e128.
29. Arantes RM, Nogueira AM. Distribution of enteroglucagon- and peptide YY-immunoreactive cells in the intestinal mucosa of germ-free and conventional mice. Cell Tissue Res 1997;290:61-69.
30. Gallego D, Hernández P, Clavé P, Jiménez M. P2Y1 receptors mediate inhibitory purinergic neuromuscular transmission in the human colon. Am J Physiol Gastrointest Liver Physiol 2006;291:G584-G594.
31. Aulí M, Martínez E, Gallego D, et al. Effects of excitatory and inhibitory neurotransmission on motor patterns of human sigmoid colon *in vitro*. Br J Pharmacol 2008;155:1043-1055.
32. Barth BB, Travis L, Spencer NJ, Grill WM. Control of colonic motility using electrical stimulation to modulate enteric neural activity. Am J Physiol Gastrointest Liver Physiol 2021;320:G675-G687.
33. Farré R, Aulí M, Lecea B, Martínez E, Clavé P. Pharmacologic characterization of intrinsic mechanisms controlling tone and relaxation of porcine lower esophageal sphincter. J Pharmacol Exp Ther 2006;316:1238-1248.
34. Erdogan BR, Karaomerlioglu I, Yesilyurt ZE, et al. Normalization of organ bath contraction data for tissue specimen size: does one approach fit all? Naunyn Schmiedebergs Arch Pharmacol 2020;393:243-251.
35. Capettini LS, Cortes SF, Gomes MA, et al. Neuronal nitric oxide synthase-derived hydrogen peroxide is a major endothelium-dependent relaxing factor. Am J Physiol Heart Circ Physiol 2008;295:H2503-H2511.
36. Santiago HC, Oliveira CF, Santiago L, et al. Involvement of the chemokine RANTES (CCL5) in resistance to experimental infection with *Leishmania major*. Infect Immun. 2004;72:4918-4923.
37. Cummings KL, Tarleton RL. Rapid quantitation of *Trypanosoma cruzi* in host tissue by real-time PCR. Mol Biochem Parasitol 2003;129:53-59.
38. Koberle F, de Alcantara F. [Mechanism of destruction of the neurons of the peripheral nervous system in Changas' disease.] Hospital (Rio J) 1960;57:1057-1062. [Portuguese]
39. Köberle F. Chagas' disease and chagas' syndromes: the pathology of American trypanosomiasis. Adv Parasitol 1968;6:63-116.
40. Arantes RM, Marche HH, Bahia MT, Cunha FQ, Rossi MA, Silva JS. Interferon-gamma-induced nitric oxide causes intrinsic intestinal denervation in *Trypanosoma cruzi*-infected mice. Am J Pathol 2004;164:1361-1368.
41. González Cappa SM, Sanz OP, Muller LA, et al. Peripheral nervous system damage in experimental chronic chagas' disease. Am J Trop Med Hyg 1987;36:41-45.
42. Guillén-Pernía B, Lugo-Yarbuh A, Moreno E. [Digestive tract dilation in mice infected with *Trypanosoma cruzi*.] Invest Clin 2001;42:195-209. [Spanish]

43. Sarna SK, Shi XZ. Function and regulation of colonic contractions in health and disease. Physiology of the Gastrointestinal Tract. Elsevier Inc. 2006.
44. Rivera LR, Poole DP, Thacker M, Furness JB. The involvement of nitric oxide synthase neurons in enteric neuropathies. Neurogastroenterol Motil 2011;23:980-988.
45. Hibberd TJ, Feng J, Luo J, et al. Optogenetic induction of colonic motility in mice. Gastroenterology 2018;155:514-528, e6.
46. Hou X, Yin J, Liu J, Pasricha PJ, Chen JD. *In vivo* gastric and intestinal slow waves in W/WV mice. Dig Dis Sci 2005;50:1335-1341.
47. Lecci A, Capriati A, Altamura M, Maggi CA. Tachykinins and tachykinin receptors in the gut, with special reference to NK2 receptors in human. Auton Neurosci 2006;126:232-249.
48. Gates TS, Zimmerman RP, Mantyh CR, et al. Substance P and substance K receptor binding sites in the human gastrointestinal tract: localization by autoradiography. Peptides 1988;9:1207-1219.
49. Venkova K, Greenwood-Van Meeveld B, Krier J. Neural control of the large intestine. Innervation of the Gastrointestinal Tract. Taylor & F. In: Brookes SJ and Costa M (eds). 2002:171-187.
50. Cellek S, Thangiah R, Bassil AK, et al. Demonstration of functional neuronal beta3-adrenoceptors within the enteric nervous system. Gastroenterology 2007;133:175-183.
51. Anand N, Paterson WG. Role of nitric oxide in esophageal peristalsis. Am J Physiol 1994;266(1 pt 1):G123-G131.
52. Boughton-Smith NK, Evans SM, Hawkey CJ, et al. Nitric oxide synthase activity in ulcerative colitis and crohn's disease. Lancet 1993;342:338-340.
53. Rachmilewitz D, Stamler JS, Bachwich D, Karmeli F, Ackerman Z, Podolsky DK. Enhanced colonic nitric oxide generation and nitric oxide synthase activity in ulcerative colitis and crohn's disease. Gut 1995;36:718-723.
54. Boeckxstaens GE, Pelckmans PA, Herman AG, Van Maercke YM. Involvement of nitric oxide in the inhibitory innervation of the human isolated colon. Gastroenterology 1993;104:690-697.
55. Keef KD, Du C, Ward SM, McGregor B, Sanders KM. Enteric inhibitory neural regulation of human colonic circular muscle: role of nitric oxide. Gastroenterology 1993;105:1009-1016.
56. Ricci MF, Campos CF, Cartelle CT, et al. Nitrergic myenteric neurons are spared in experimental Chagasic megacolon. J Neuroinfectious Dis 2016;7:235.
57. Seifi M, Brown JF, Mills J, et al. Molecular and functional diversity of GABA-A receptors in the enteric nervous system of the mouse colon. J Neurosci 2014;34:10361-10378.
58. Blennerhassett MG, Vignjevic P, Vermillion DL, Collins SM. Inflammation causes hyperplasia and hypertrophy in smooth muscle of rat small intestine. Am J Physiol 1992;262(6 pt 1):G1041-G1046.
59. Blennerhassett MG, Bovell FM, Lourenssen S, McHugh KM. Characteristics of inflammation-induced hypertrophy of rat intestinal smooth muscle cell. Dig Dis Sci 1999;44:1265-1272.
60. Unno T, Matsuyama H, Izumi Y, Yamada M, Wess J, Komori S. Roles of M2 and M3 muscarinic receptors in cholinergic nerve-induced contractions in mouse ileum studied with receptor knockout mice. Br J Pharmacol 2006;149:1022-1030.
61. Ochillo RF, Tsai CS. A comparative study of the effects of aging on the responsiveness of the cholinergic receptor of the isolated ileum of mouse and rat. Res Commun Chem Pathol Pharmacol 1988;60:261-264.
62. Ben-Horin S, Chowers Y. Neuroimmunology of the gut: physiology, pathology, and pharmacology. Curr Opin Pharmacol 2008;8:490-495.
63. Schliebs R, Arendt T. The cholinergic system in aging and neuronal degeneration. Behav Brain Res 2011;221:555-563.
64. Nordberg A. Human nicotinic receptors--their role in aging and dementia. Neurochem Int 1994;25:93-97.
65. Montedonico S, Sri Paran T, Pirker M, Rolle U, Puri P. Developmental changes in submucosal nitrergic neurons in the porcine distal colon. J Pediatr Surg 2006;41:1029-1035.